Extracting the Energy-Dependent Neutrino-Nucleon Cross Section above 10 TeV Using IceCube Showers

Mauricio Bustamante[1,2,3,*] and Amy Connolly[2,3,†]

[1]*Niels Bohr International Academy & Discovery Centre, Niels Bohr Institute, Blegdamsvej 17, 2100 Copenhagen, Denmark*
[2]*Center for Cosmology and AstroParticle Physics (CCAPP), The Ohio State University, Columbus, Ohio 43210, USA*
[3]*Department of Physics, The Ohio State University, Columbus, Ohio 43210, USA*

Neutrinos are key to probing the deep structure of matter and the high-energy Universe. Yet, until recently, their interactions had only been measured at laboratory energies up to about 350 GeV. An opportunity to measure their interactions at higher energies opened up with the detection of high-energy neutrinos in IceCube, partially of astrophysical origin. Scattering off matter inside Earth affects the distribution of their arrival directions—from this, we extract the neutrino-nucleon cross section at energies from 18 TeV to 2 PeV, in four energy bins, in spite of uncertainties in the neutrino flux. Using six years of public IceCube High-Energy Starting Events, we explicitly show for the first time that the energy dependence of the cross section above 18 TeV agrees with the predicted softer-than-linear dependence, and reaffirm the absence of new physics that would make the cross section rise sharply, up to a center-of-mass energy $\sqrt{s} \approx 1$ TeV.

Introduction.—Neutrino interactions, though feeble, are important for particle physics and astrophysics. They provide precise tests of the standard model [1–3], probes of new physics [4–6], and windows to otherwise veiled regions of the Universe. Yet, at neutrino energies above 350 GeV there had been no measurement of their interactions. This changed recently when the IceCube Collaboration found that the neutrino-nucleon cross section from 6.3 to 980 TeV agrees with predictions [7].

Because there is no artificial neutrino beam at a TeV and above, IceCube used atmospheric and astrophysical neutrinos, the latter discovered by them up to a few PeV [8–16]. References [4,6,17–20] showed that, because IceCube neutrinos interact significantly with matter inside Earth, their distribution in energy and arrival direction carries information about neutrino-nucleon cross sections, which, like IceCube [7], we extract.

However, Ref. [7] extracted the cross section in a single, wide energy bin, so its energy dependence in that range remains untested. A significant deviation from the predicted softer-than-linear dependence could signal the presence of new physics, so we extract the cross section in intervals from 18 TeV to 2 PeV. While Ref. [7] used only events born outside of IceCube we use instead only events born inside of it, which leads to a better handle on the neutrino energy.

Figure 1 shows that the cross section that we extract is compatible with the standard prediction. There is no indication of the sharp rise, at least below 1 PeV, predicted by some models of new physics [6,21–29].

Neutrino-nucleon cross section.—Above a few GeV, neutrino-nucleon interactions are typically deep inelastic
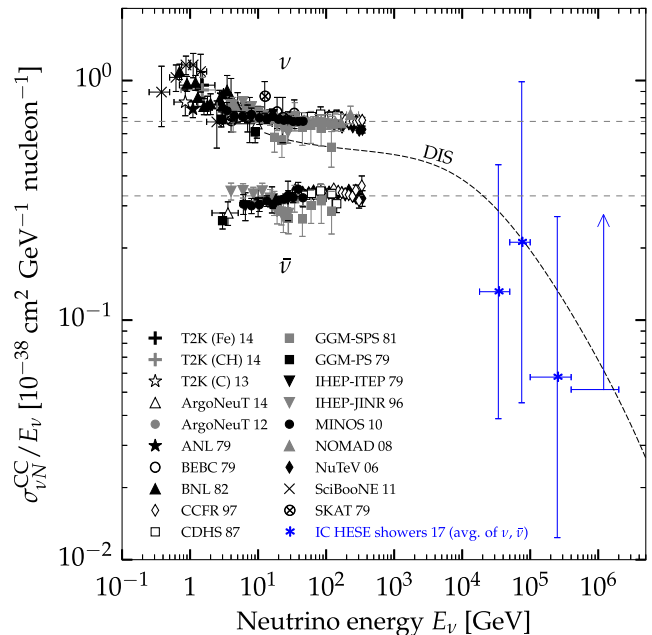

FIG. 1. Charged-current inclusive neutrino-nucleon cross section measurements [30–47]. The new results from this work, based on 6 years of IceCube HESE showers [8,48–50], are an average between cross sections for ν and $\bar{\nu}$, assuming equal astrophysical fluxes of each. In the highest-energy bin, we only set a lower limit (1σ shown). The thick dashed curve is a standard prediction of deep inelastic scattering (DIS), averaged between ν and $\bar{\nu}$. Horizontal thin dashed lines are global averages from Ref. [51], which do not include the new results.

scatterings (DIS), where the neutrino scatters off one of the constituent partons of the nucleon—a quark or a gluon. In both the charged-current (CC, $\overset{(-)}{\nu}_l + N \to l^{\mp} + X$) and neutral-current (NC, $\overset{(-)}{\nu}_l + N \to \overset{(-)}{\nu}_l + X$) forms of this interaction, the nucleon N is broken up into partons that hadronize into a final state X. The final-state hadrons carry a fraction y—the inelasticity—of the initial neutrino energy, while the final-state lepton carries the remaining fraction $(1 - y)$.

Calculation of the cross section $\sigma_{\nu N}$ requires knowing the parton distribution functions (PDFs) in the nucleon. PDFs depend on two kinematic variables: $Q^2 \equiv -q^2$, the four-momentum transferred to the mediating W or Z boson, and the Bjorken scaling x, the fraction of nucleon momentum carried by the interacting parton [52].

To compute cross sections at neutrino energies E_ν between TeV and PeV, we need PDFs evaluated at $x \gtrsim m_W/E_\nu \sim 10^{-4}$. Because these are known—at low x, from ep collisions in HERA [53,54]—the uncertainty in the predicted TeV-PeV cross sections is small. References [4,55–65] have performed such calculations, some of which are shown in Fig. 3. Below ~10 TeV, they yield $\sigma_{\nu N} \propto E_\nu$, revelatory of hard scattering off partons, and in agreement with data. Above ~10 TeV, where $Q^2 \sim m_W^2$, they yield a softer-than-linear energy dependence, which has only been glimpsed in the available data up to 350 GeV [1–3].

Detecting high-energy neutrinos.—IceCube is the largest optical-Cherenkov neutrino detector. It consists of strings of photomultipliers buried deep in the clear Antarctic ice, instrumenting a volume of about 1 km³.

Above TeV, CC interactions of ν_e and ν_τ with nucleons in the ice, and NC interactions of all flavors, create localized particle showers, with roughly spherical Cherenkov-light profiles centered on the interaction vertex. CC interactions of ν_μ additionally create muons that make elongated tracks of Cherenkov light, several kilometers long and easily identifiable. (Other, flavor-specific signatures require energies higher than in our analysis [66–74].)

From the amount of collected light in a detected event, and its spatial and temporal profiles, IceCube infers its energy and arrival direction. But it cannot distinguish neutrinos from antineutrinos, or NC from CC showers, since they make similar light signals.

Using contained showers only.—Because cross sections vary with neutrino energy, we use exclusively a class of IceCube events where the incoming neutrino energy can be inferred using as few assumptions as possible. These are "starting events," where the neutrino interaction was contained in the detector. Of these, we use only showers, not tracks, due not to a fundamental limitation, but to the IceCube data that is publicly available. Our approach differs from that of Ref. [7], which used only through-going muons, born in neutrino interactions outside the

detector, for which estimation of the neutrino energy requires making important assumptions.

We use the publicly available 6-year sample of IceCube High-Energy Starting Events (HESE) [8,48–50], consisting of 58 contained showers with deposited energies E_{dep} from 18 TeV to 2 PeV. Below a few tens of TeV, about half of the showers are due to atmospheric neutrinos and half to astrophysical neutrinos [50]; above, showers from astrophysical neutrinos dominate [75,76].

Figure 2 shows the HESE showers distributed in E_{dep} and zenith angle θ_z. Representative uncertainties are 10% in E_{dep} and 15° in θ_z [77], which we adopt to describe the detector resolution. Showers are scarce above 200 TeV because the neutrino flux falls steeply with E_ν.

In CC showers, the full neutrino energy is deposited in the ice, i.e., $E_{dep} \approx E_\nu$, because both the outgoing electron or tau and the final-state hadrons shower. In NC showers, only a fraction y of the neutrino energy is deposited in the ice, i.e., $E_{dep} = y E_\nu$, because only final-state hadrons shower. Standard calculations yield an average $\langle y \rangle = 0.35$ at 10 TeV and 0.25 at 1 PeV [55]. Because of this low value and because the neutrino fluxes fall steeply with E_ν, NC showers are nominally subdominant at any value of E_{dep}.

In starting tracks, the shower made by final-state hadrons is contained by the detector, but the muon track typically exits
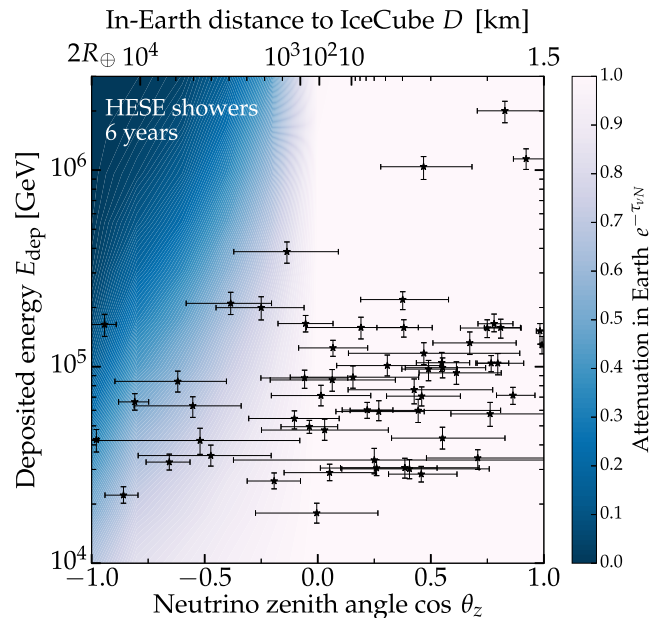

FIG. 2. Neutrino-induced showers from the IceCube 6-year HESE [8,48–50] sample. Neutrinos arrive from above ($\cos\theta_z > 0$); from below, through Earth ($\cos\theta_z < 0$); and horizontally ($\cos\theta_z = 0$). They travel a distance D inside Earth (of radius $R_\oplus = 6371$ km) to IceCube, buried at a depth of 1.5 km. The background shading represents the fraction of isotropic neutrino flux that survives after being attenuated by νN interactions inside Earth, calculated using cross sections predicted in Ref. [59].

it. An assumption-free reconstruction of E_ν requires knowing separately the energy of the hadronic shower $E_{\rm sh}$ and the muon energy loss rate dE_μ/dX, which is proportional to the muon energy E_μ [77]. Yet, while these quantities are known internally to the IceCube Collaboration, public data only provide, for each starting track, the total deposited energy, $E_{\rm sh} + |dE_\mu/dX|\Delta X$, where ΔX is the track length in the detector. Without additional information, in order to deduce E_ν, we would need to assume values of y and ΔX for each event [78]. Hence, in keeping to our tenet of using few assumptions to deduce E_ν, we do not include starting tracks in our analysis. This choice also reduces the chance of erroneously using a track created by an atmospheric muon, not a neutrino.

To use through-going muons in extracting the cross section, IceCube [7] inferred the most likely parent neutrino energy from the measured muon energy [77] by assuming the inelasticity distribution $d\sigma_{\nu N}/dy$ from Ref. [59]. By using only contained showers, we forgo the need to assume an inelasticity distribution, and remain more sensitive to potential new physics that could modify it.

Sensitivity to the cross section.—Neutrino-nucleon interactions make Earth opaque to neutrinos above 10 TeV, so neutrino fluxes are attenuated upon reaching IceCube. More neutrinos reach it from above—after crossing a few kilometers of ice—than from below—after crossing up to the diameter of Earth.

A flux of incoming neutrinos with energy E_ν and zenith angle θ_z is attenuated by a factor $e^{-\tau_{\nu N}(E_\nu, \theta_z)} \equiv \exp[-D(\theta_z)/L_{\nu N}(E_\nu, \theta_z)]$, where $\tau_{\nu N}$ is the opacity to νN interactions, D is the distance from the point of entry into Earth to IceCube, and $L_{\nu N} = m_N/[(\sigma_{\nu N}^{\rm CC}(E_\nu) + \sigma_{\nu N}^{\rm NC}(E_\nu))\langle\rho_\oplus(\theta_z)\rangle]$ is the neutrino interaction length. Here, $\sigma_{\nu N}^{\rm CC}$ and $\sigma_{\nu N}^{\rm NC}$ are, respectively, the CC and NC cross sections, m_N is the average nucleon mass in isoscalar matter, and $\langle\rho_\oplus\rangle$ is the average matter density along this direction, calculated using the density profile from the preliminary reference Earth model [55,79]. Details are in the Supplemental Material [80], which includes Refs. [81–94]. Attenuation grows with the cross sections—which grow with E_ν—and with D; both effects are evident in the background shading in Fig. 2.

Within an energy interval, the number of events induced by a neutrino flux Φ_ν is $N_{\rm sh} \propto \Phi_\nu e^{-\tau_{\nu N}}\sigma_{\nu N}$. Down-going showers ($\cos\theta_z > 0$)—unaffected by attenuation—fix the product $\Phi_\nu\sigma_{\nu N}$, while up-going showers ($\cos\theta_z < 0$)—affected by attenuation—break the degeneracy between Φ_ν and $\sigma_{\nu N}$ via $e^{-\tau_{\nu N}}$, providing sensitivity to the cross sections.

Extracting cross sections.—We propagate atmospheric and astrophysical neutrinos through Earth and produce test samples of contained showers in IceCube, taking into account its energy and angular resolution; see the Supplemental Material [80]. To extract the cross sections, we compare the distributions in $E_{\rm dep}$ and $\cos\theta_z$ of the test showers—generated with varying values of the cross sections—to the distribution observed by IceCube.

To probe the energy dependence of the cross sections, we bin showers in $E_{\rm dep}$ and extract the cross section from data in each bin independently of the others. Except for global assumptions on detector resolution and the choice of atmospheric neutrino spectrum (see below), parameters extracted in different bins are uncorrelated.

The first three bins contain comparable numbers of showers: 18–50 TeV (17 showers), 50–100 TeV (18 showers), and 100–400 TeV (20 showers). The final bin, 400–2004 TeV, contains only 3 downgoing showers, between 1–2 PeV. Because of their short travel distances ($D \lesssim 10$ km) and negligible expected attenuation, in this bin we only set a lower limit on the cross section. This stresses the need for upgoing HESE events above 400 TeV.

For atmospheric neutrinos, we use the most recent calculation of the ν_e, $\bar{\nu}_e$, ν_μ, and $\bar{\nu}_\mu$ fluxes from pion and kaon decays from Ref. [95]. Their zenith-angle distribution at the South Pole, though anisotropic, is symmetric around $\cos\theta_z = 0$, so it does not introduce spurious directional asymmetries. We do not include a contribution from prompt atmospheric neutrinos [96–109], since searches have failed to find evidence of them [8–16]. We include the self-veto [110,111] used by the HESE analysis to reduce the atmospheric contribution.

For astrophysical neutrinos, we assume, independently in each energy bin, an isotropic power-law energy spectrum $\Phi_\nu \propto E_\nu^{-\gamma}$ for all flavors of neutrinos and antineutrinos, in agreement with theoretical expectations [112] and IceCube findings [113]. The value of γ is obtained from a fit to data in each bin. This makes our results robust against variations with energy of the spectral shape of astrophysical neutrinos, unlike Ref. [7], which assumed a single power law spanning the range 6.3–980 TeV. We assume flavor equipartition, as expected from standard mixing [68,78,114–118] and in agreement with data [14,119]. Because IceCube cannot distinguish neutrinos from antineutrinos, we can only extract a combination of their cross sections, each weighed by its corresponding flux. We assume the likely case [120,121] of equal fluxes, coming, e.g., from proton-proton interactions [122].

Assumptions.—Because data are scant, to reduce the number of free parameters to fit, we make three reasonable assumptions inspired on standard high-energy predictions. With more data, they could be tested.

First, the rate of CC showers dominates over the rate of NC showers at any value of $E_{\rm dep}$, based on the arguments above. For simplicity, we adopt a constant $\langle y \rangle = 0.25$ for NC showers. This assumption allows us to express the extracted cross section as a function of $E_\nu \approx E_{\rm dep}$.

Second, CC cross sections dominate over NC cross sections. We assume $\sigma_{\nu N}^{\rm NC} = \sigma_{\nu N}^{\rm CC}/3$ and $\sigma_{\bar{\nu} N}^{\rm NC} = \sigma_{\bar{\nu} N}^{\rm CC}/3$, following, e.g., Ref. [4]. This assumption allows us to fit only for CC cross sections.

Third, the ratio of $\bar{\nu} N$ to νN cross sections is fixed in each bin. Hence, when fitting, $\sigma_{\bar{\nu} N}^{\rm CC} = \langle \sigma_{\bar{\nu} N}^{\rm CC}/\sigma_{\nu N}^{\rm CC}\rangle\sigma_{\nu N}^{\rm CC}$,

TABLE I. Neutrino-nucleon charged-current inclusive cross sections, averaged between neutrinos ($\sigma_{\nu N}^{CC}$) and antineutrinos ($\sigma_{\bar{\nu} N}^{CC}$), extracted from 6 years of IceCube HESE showers. To obtain these results, we fixed $\sigma_{\bar{\nu} N}^{CC} = \langle \sigma_{\bar{\nu} N}^{CC}/\sigma_{\nu N}^{CC} \rangle \sigma_{\nu N}^{CC}$—where $\langle \sigma_{\bar{\nu} N}^{CC}/\sigma_{\nu N}^{CC} \rangle$ is the average ratio of $\bar{\nu}$ to ν cross sections calculated using the standard prediction from Ref. [59]—and $\sigma_{\nu N}^{NC} = \sigma_{\nu N}^{CC}/3$, $\sigma_{\bar{\nu} N}^{NC} = \sigma_{\bar{\nu} N}^{CC}/3$. Uncertainties are 1σ, statistical plus systematic, added in quadrature.

E_ν [TeV]	$\langle E_\nu \rangle$ [TeV]	$\langle \sigma_{\bar{\nu} N}^{CC}/\sigma_{\nu N}^{CC} \rangle$	$\log_{10}[\frac{1}{2}(\sigma_{\nu N}^{CC}+\sigma_{\bar{\nu} N}^{CC})/\mathrm{cm}^2]$
18–50	32	0.752	-34.35 ± 0.53
50–100	75	0.825	-33.80 ± 0.67
100–400	250	0.888	-33.84 ± 0.67
400–2004	1202	0.957	$> -33.21(1\sigma)$

where $\langle \sigma_{\bar{\nu} N}^{CC}/\sigma_{\nu N}^{CC} \rangle$ is the average ratio in that bin predicted by Ref. [59] (see Table I). This assumption allows us to fit only for νN cross sections.

Thus, within each energy bin, we independently vary only the νN CC cross section $\sigma_{\nu N}^{CC}$ and three nuisance parameters—the number of showers due to atmospheric neutrinos N_{sh}^{atm}, the number of showers due to astrophysical neutrinos N_{sh}^{ast}, and the astrophysical spectral index γ. To avoid introducing bias, we assume flat priors for all of them. For each choice of values, we compare our test shower spectrum to the HESE shower spectrum via a likelihood. To find the best-fit values of the parameters, we maximize the likelihood. The Supplemental Material describes the statistical analysis in detail [80].

Results.—Table I shows the extracted cross section, marginalized over the nuisance parameters. Because $\sigma_{\nu N}$ and $\sigma_{\bar{\nu} N}$ are not independent in the fit, we present their average there and in Figs. 2 and 3.

Figure 3 shows that, in each bin, results agree within 1σ with widely used standard predictions. The IceCube Collaboration has adopted the cross section from Cooper-Sarkar *et al.* [59]. We include other calculations for comparison [4,55,56,60,62]. All predictions are consistent with our measurements within errors.

Our results are consistent with the IceCube analysis [7], which found a cross section compatible with Ref. [59]. Their smaller uncertainty is due to using $\sim 10^4$ through-going muons. However, by grouping all events in a single energy bin, their analysis did not probe the energy dependence of the cross section. Like that analysis, our results are also consistent with standard cross-section predictions, but in narrower energy intervals.

Because the number of showers in each bin is small, statistical fluctuations weaken the interplay of down-going versus up-going showers described above. To isolate the dominant statistical uncertainty, we minimized again the likelihood, this time keeping the nuisance parameters fixed at their best-fit values (see Table II in the Supplemental Material [80]). The resulting uncertainty, attributed to statistics only, is
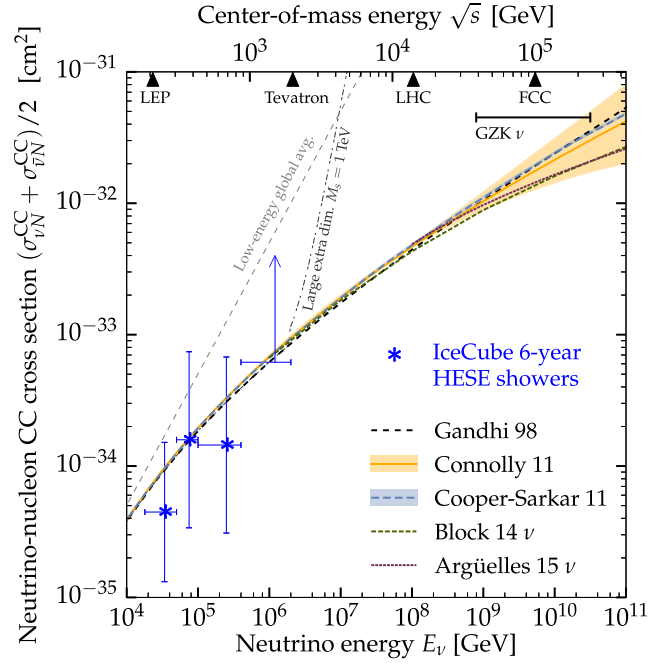

FIG. 3. Neutrino-nucleon charged-current cross section, averaged for neutrinos and antineutrinos, from different predictions (lines) [4,56,59,60,62], compared to measurements from this work (stars). The low-energy global average [51] has the linear dependence on E_ν appropriate below ~ 10 TeV. The model of large extra dimensions, included for illustration, is from Ref. [21] (quantum-gravity scale of 1 TeV and all partial waves summed), corrected here to match modern standard predictions of the cross section below 1 PeV.

0.51, 0.63, and 0.62 in the first three bins, where we have a measurement. The systematic uncertainty, obtained by subtracting these values in quadrature from the total uncertainties in Table I is 0.14, 0.23, and 0.25 in each bin, slightly higher than in Ref. [7], due to a less detailed modeling of the detector. While Ref. [7] found comparable statistical and systematic uncertainties, we are presently dominated by statistics, since it uses an event sample that is smaller by a factor of ~ 200.

Nevertheless, our results disfavor new-physics models where the cross section rises sharply below 1 PeV [6,22–29]. Figure 3 shows as example a model of TeV-scale gravity with large extra dimensions [21]. While this model was disfavored by the LHC [123,124], we provide independent confirmation via a different channel. More stringent tests of new-physics models, beyond the scope of this Letter, should also consider the effect of modifications to the inelasticity distribution.

Limitations and improvements.—IceCube is sparsely instrumented and designed to detect the enormous light imprints made by high-energy neutrinos. Except for high-energy muons, it cannot track individual particles or reconstruct Q^2 and x, unlike densely instrumented detectors. Hence, we can only extract the cross section as a

function of energy, integrated over other kinematic variables. While we cannot extract individual PDFs, we can test their combination in the cross section.

Further, IceCube cannot distinguish if a particular shower was made in a CC or an NC interaction, and by a neutrino or an antineutrino. The differences are too subtle to unequivocally identify them in individual showers [125], but it might be possible to extract them statistically from a large enough data sample [126].

Lastly, we assumed that the astrophysical neutrino flux is isotropic [14,127,128]. Nevertheless, there are hints of a Galactic contribution [14,127,129,130], with data allowing $< 14\%$ of the all-sky flux to come from the Galactic Plane [128]. If a Galactic flux is discovered, future cross-section analyses will need to acknowledge its anisotropy to avoid incorrectly attributing the distribution of arrival directions solely to in-Earth attenuation.

Summary and outlook.—We have extracted the energy dependence of the neutrino-nucleon cross section at energies beyond those available in man-made neutrino beams, making use of the high-energy reach of IceCube. Our results are compatible with predictions based on nucleon structure extracted from scattering experiments at lower energies and disfavor extreme deviations that could stem from new physics in the TeV–PeV range.

It would be straightforward to repeat the present analysis using a larger HESE shower sample. The proposed upgrade IceCube-Gen2 [131] could have an event rate 5–7 times higher, thus reducing the impact of random fluctuations. These showers could be combined with showers from the upcoming KM3NeT detector [132]; their improved angular resolution of $\sim 2°$ above 50 TeV would allow for better estimates of in-Earth attenuation. Starting tracks can also be considered, as long as one does not rely on predictions of the inelasticity distribution to reconstruct the parent neutrino energy.

An interesting possibility is to measure the inelasticity distribution [133]. This can be done using starting tracks where the hadronic shower energy E_{sh} and the outgoing muon energy E_μ are known individually, in order to reconstruct the inelasticity $y = (1 + E_\mu / E_{sh})^{-1}$ [134,135].

At the EeV scale, differences between cross-section predictions increase. Measuring $\sigma_{\nu N}$ at these energies would probe $x \sim m_W / E_\nu \lesssim 10^{-6}$, beyond the reach of laboratory scattering experiments. This would prove instrumental in testing not only new physics, but also predictions of the potentially nonlinear behavior of PDFs at low x, such as from BFKL theory [136–139] and color-glass condensates [140]; see, e.g., Refs. [63,141,142]. However, because the predicted neutrino flux at these energies, while uncertain, is smaller than at PeV, precision measurements of the cross section will likely be limited by statistics; see Ref. [143] for details. Nevertheless, large-volume neutrino detectors like ARA [144–146], ARIANNA [147,148], GRAND [149], and POEMMA [150] might differentiate [151] between predictions provided the event rate is high enough.

---

[*]mbustamante@nbi.ku.dk; ORCID: 0000-0001-6923-0865
[†]connolly@physics.osu.edu; ORCID: 0000-0003-0049-5448

[1] R. Brock *et al.* (CTEQ Collaboration), Handbook of perturbative QCD: Version 1.0, Rev. Mod. Phys. **67**, 157 (1995).
[2] J. M. Conrad, M. H. Shaevitz, and T. Bolton, Precision measurements with high-energy neutrino beams, Rev. Mod. Phys. **70**, 1341 (1998).
[3] J. A. Formaggio and G. P. Zeller, From eV to EeV: Neutrino cross sections across energy scales, Rev. Mod. Phys. **84**, 1307 (2012).
[4] A. Connolly, R. S. Thorne, and D. Waters, Calculation of high energy neutrino-nucleon cross sections and uncertainties using the MSTW parton distribution functions and implications for future experiments, Phys. Rev. D **83**, 113009 (2011).
[5] C.-Y. Chen, P. S. Bhupal Dev, and A. Soni, Standard model explanation of the ultrahigh energy neutrino events at IceCube, Phys. Rev. D **89**, 033012 (2014).
[6] D. Marfatia, D. W. McKay, and T. J. Weiler, New physics with ultra-high-energy neutrinos, Phys. Lett. B **748**, 113 (2015).
[7] M. G. Aartsen *et al.* (IceCube Collaboration), Measurement of the multi-TeV neutrino cross section with IceCube using Earth absorption, Nature (London) **551**, 596 (2017).
[8] M. G. Aartsen *et al.* (IceCube Collaboration), Observation of High-Energy Astrophysical Neutrinos in Three Years of IceCube Data, Phys. Rev. Lett. **113**, 101101 (2014).
[9] M. G. Aartsen *et al.* (IceCube Collaboration), First Observation of PeV-Energy Neutrinos with IceCube, Phys. Rev. Lett. **111**, 021103 (2013).
[10] M. G. Aartsen *et al.* (IceCube Collaboration), Evidence for high-energy extraterrestrial neutrinos at the IceCube detector, Science **342**, 1242856 (2013).
[11] M. G. Aartsen *et al.* (IceCube Collaboration), Search for a diffuse flux of astrophysical muon neutrinos with the IceCube 59-string configuration, Phys. Rev. D **89**, 062007 (2014).
[12] M. G. Aartsen *et al.* (IceCube Collaboration), Atmospheric and astrophysical neutrinos above 1 TeV interacting in IceCube, Phys. Rev. D **91**, 022001 (2015).
[13] M. G. Aartsen *et al.* (IceCube Collaboration), Measurement of the atmospheric ν_e spectrum with IceCube, Phys. Rev. D **91**, 122004 (2015).

[14] M. G. Aartsen *et al.* (IceCube Collaboration), A combined maximum-likelihood analysis of the high-energy astrophysical neutrino flux measured with IceCube, Astrophys. J. **809**, 98 (2015).

[15] M. G. Aartsen *et al.* (IceCube Collaboration), Evidence for Astrophysical Muon Neutrinos from the Northern Sky with IceCube, Phys. Rev. Lett. **115**, 081102 (2015).

[16] M. G. Aartsen *et al.* (IceCube Collaboration), Observation and characterization of a cosmic muon neutrino flux from the northern hemisphere using six years of IceCube data, Astrophys. J. **833**, 3 (2016).

[17] D. Hooper, Measuring high-energy neutrino nucleon cross-sections with future neutrino telescopes, Phys. Rev. D **65**, 097303 (2002).

[18] S. Hussain, D. Marfatia, D. W. McKay, and D. Seckel, Cross Section Dependence of Event Rates at Neutrino Telescopes, Phys. Rev. Lett. **97**, 161101 (2006).

[19] E. Borriello, A. Cuoco, G. Mangano, G. Miele, S. Pastor, O. Pisanti, and P. D. Serpico, Disentangling neutrino-nucleon cross section and high energy neutrino flux with a km^3 neutrino telescope, Phys. Rev. D **77**, 045019 (2008).

[20] S. Hussain, D. Marfatia, and D. W. McKay, Upward shower rates at neutrino telescopes directly determine the neutrino flux, Phys. Rev. D **77**, 107304 (2008).

[21] J. Alvarez-Muniz, F. Halzen, Tao Han, and D. Hooper, Phenomenology of High-Energy Neutrinos in Low Scale Quantum Gravity Models, Phys. Rev. Lett. **88**, 021301 (2001).

[22] J. Alvarez-Muniz, J. L. Feng, F. Halzen, T. Han, and D. Hooper, Detecting microscopic black holes with neutrino telescopes, Phys. Rev. D **65**, 124015 (2002).

[23] L. A. Anchordoqui, J. L. Feng, H. Goldberg, and A. D. Shapere, Updated limits on TeV scale gravity from absence of neutrino cosmic ray showers mediated by black holes, Phys. Rev. D **68**, 104025 (2003).

[24] E.-J. Ahn, M. Cavaglia, and A. V. Olinto, Uncertainties in limits on TeV gravity from neutrino induced air showers, Astropart. Phys. **22**, 377 (2005).

[25] J. I. Illana, M. Masip, and D. Meloni, Cosmogenic Neutrinos and Signals of TeV Gravity in Air Showers and Neutrino Telescopes, Phys. Rev. Lett. **93**, 151102 (2004).

[26] S. Hussain and D. W. McKay, Bounds on low scale gravity from RICE data and cosmogenic neutrino flux models, Phys. Lett. B **634**, 130 (2006).

[27] L. A. Anchordoqui, M. M. Glenz, and L. Parker, Black holes at IceCube neutrino telescope, Phys. Rev. D **75**, 024011 (2007).

[28] J. Lykken, O. Mena, and S. Razzaque, Ultrahigh-energy neutrino flux as a probe of large extra-dimensions, J. Cosmol. Astropart. Phys. 12 (2007) 015.

[29] L. A. Anchordoqui, H. Goldberg, D. Gora, T. Paul, M. Roth, S. Sarkar, and L. L. Winders, Using cosmic neutrinos to search for non-perturbative physics at the Pierre Auger Observatory, Phys. Rev. D **82**, 043001 (2010).

[30] A. I. Mukhin *et al.*, Energy dependence of total cross-sections for neutrino and anti-neutrino interactions at energies below 35-GeV, Yad. Fiz. **30**, 1014 (1979) [Sov. J. Nucl. Phys. **30**, 528 (1979)].

[31] D. S. Baranov *et al.*, Measurements of the $\nu_\mu N$ total cross section at 2-GeV–30-GeV in SKAT neutrino experiment, Phys. Lett. **81B**, 255 (1979).

[32] S. J. Barish, M. Derrick, T. Dombeck, L. G. Hyman, K. Jaeger, B. Musgrave, P. Schreiner, R. Singer, A. Snyder, V. E. Barnes, D. D. Carmony, and A. F. Garfinkel, Study of neutrino interactions in hydrogen and deuterium: Inelastic charged current reactions, Phys. Rev. D **19**, 2521 (1979).

[33] S. Ciampolillo *et al.* (Aachen-Brussels-CERN-Ecole Poly-Orsay-Padua, Gargamelle Neutrino Propane Collaboration), Total cross-section for neutrino charged current interactions at 3-GeV and 9-GeV, Phys. Lett. B **84**, 281 (1979).

[34] J. G. H. de Groot *et al.*, Inclusive interactions of high-energy neutrinos and anti-neutrinos in Iron, Z. Phys. C **1**, 143 (1979).

[35] D. C. Colley *et al.*, Cross-sections for charged current neutrino and anti-neutrino interactions in the energy range 10-GeV to 50-GeV, Z. Phys. C **2**, 187 (1979).

[36] J. G. Morfin *et al.* (Gargamelle SPS Collaboration), Total cross-sections and nucleon structure functions in the Gargamelle SPS neutrino/anti-neutrino experiment, Phys. Lett. **104B**, 235 (1981).

[37] N. J. Baker, P. L. Connolly, S. A. Kahn, M. J. Murtagh, R. B. Palmer, N. P. Samios, and M. Tanaka, Total cross-sections for muon-neutrino N and muon-neutrino P charged current interactions in the 7-ft bubble chamber, Phys. Rev. D **25**, 617 (1982).

[38] J. P. Berge *et al.*, Total neutrino and anti-neutrino charged current cross-section measurements in 100-GeV, 160-GeV and 200-GeV narrow band beams, Z. Phys. C **35**, 443 (1987).

[39] V. B. Anikeev *et al.*, Total cross-section measurements for muon-neutrino, anti-muon-neutrino interactions in 3-GeV–30-GeV energy range with IHEP-JINR neutrino detector, Z. Phys. C **70**, 39 (1996).

[40] W. G. Seligman, A Next-to-leading order QCD analysis of neutrino-iron structure functions at the tevatron, Ph.D. thesis, Columbia University, 1997.

[41] M. Tzanov *et al.* (NuTeV Collaboration), Precise measurement of neutrino and anti-neutrino differential cross sections, Phys. Rev. D **74**, 012008 (2006).

[42] Q. Wu *et al.* (NOMAD Collaboration), A precise measurement of the muon neutrino-nucleon inclusive charged current cross-section off an isoscalar target in the energy range $2.5 < E_\nu < 40$ GeV by NOMAD, Phys. Lett. B **660**, 19 (2008).

[43] P. Adamson *et al.* (MINOS Collaboration), Neutrino and antineutrino inclusive charged-current cross section measurements with the MINOS near detector, Phys. Rev. D **81**, 072002 (2010).

[44] Y. Nakajima *et al.* (SciBooNE Collaboration), Measurement of inclusive charged current interactions on carbon in a few-GeV neutrino beam, Phys. Rev. D **83**, 012005 (2011).

[45] K. Abe *et al.* (T2K Collaboration), Measurement of the inclusive ν_μ charged current cross section on carbon in the near detector of the T2K experiment, Phys. Rev. D **87**, 092003 (2013).

[46] R. Acciarri *et al.* (ArgoNeuT Collaboration), Measurements of inclusive muon neutrino and antineutrino charged current differential cross sections on argon in the NuMI antineutrino beam, Phys. Rev. D **89,** 112003 (2014).

[47] K. Abe *et al.* (T2K Collaboration), Measurement of the inclusive ν_μ charged current cross section on iron and hydrocarbon in the T2K on-axis neutrino beam, Phys. Rev. D **90,** 052010 (2014).

[48] C. Kopper, W. Giang, and N. Kurahashi (IceCube Collaboration), Observation of astrophysical neutrinos in four years of IceCube data, Proc. Sci, ICRC2015 (**2016**) 1081.

[49] IceCube Collaboration, *Observation of Astrophysical Neutrinos in Four Years of IceCube Data* (2015).

[50] Claudio Kopper, Observation of astrophysical neutrinos in six years of IceCube data, Proc. Sci. ICRC2017 (**2018**) 981.

[51] C. Patrignani *et al.* (Particle Data Group), Review of particle physics, Chin. Phys. C **40,** 100001 (2016).

[52] C. Giunti and C. W. Kim, *Fundamentals of Neutrino Physics and Astrophysics* (Oxford University Press, Oxford, 2007).

[53] F. D. Aaron *et al.* (ZEUS and H1 Collaborations), Combined measurement and QCD analysis of the inclusive $e^{+-}p$ scattering cross sections at HERA, J. High Energy Phys. 01 (2010) 109.

[54] H. Abramowicz *et al.* (ZEUS and H1 Collaborations), Combination of measurements of inclusive deep inelastic $e^\pm p$ scattering cross sections and QCD analysis of HERA data, Eur. Phys. J. C **75,** 580 (2015).

[55] R. Gandhi, C. Quigg, M. H. Reno, and I. Sarcevic, Ultrahigh-energy neutrino interactions, Astropart. Phys. **5,** 81 (1996).

[56] R. Gandhi, C. Quigg, M. H. Reno, and I. Sarcevic, Neutrino interactions at ultrahigh energies, Phys. Rev. D **58,** 093009 (1998).

[57] A. C.-Sarkar and S. Sarkar, Predictions for high energy neutrino cross-sections from the ZEUS global PDF fits, J. High Energy Phys. 01 (2008) 075.

[58] M. Gluck, P. Jimenez-Delgado, and E. Reya, Charged current neutrino-nucleon total cross section at high energies, Phys. Rev. D **81,** 097501 (2010).

[59] A. C.-Sarkar, P. Mertsch, and S. Sarkar, The high energy neutrino cross-section in the Standard Model and its uncertainty, J. High Energy Phys. 08 (2011) 042.

[60] M. M. Block, L. Durand, and P. Ha, Connection of the virtual $\gamma^* p$ cross section of ep deep inelastic scattering to real γp scattering, and the implications for νN and $e p$ total cross sections, Phys. Rev. D **89,** 094027 (2014).

[61] V. P. Goncalves and D. R. Gratieri, Estimating nonlinear QCD effects in ultrahigh energy neutrino events at IceCube, Phys. Rev. D **90,** 057502 (2014).

[62] C. A. Arguelles, F. Halzen, L. Wille, M. Kroll, and M. H. Reno, High-energy behavior of photon, neutrino, and proton cross sections, Phys. Rev. D **92,** 074040 (2015).

[63] J. L. Albacete, J. I. Illana, and A. Soto-Ontoso, Neutrino-nucleon cross section at ultrahigh energy and its astrophysical implications, Phys. Rev. D **92,** 014027 (2015).

[64] R. Gauld and J. Rojo, Precision Determination of the Small-x Gluon from Charm Production at LHCb, Phys. Rev. Lett. **118,** 072001 (2017).

[65] R. D. Ball, V. Bertone, M. Bonvini, S. Marzani, J. Rojo, and L. Rottoli, Parton distributions with small-x resummation: Evidence for BFKL dynamics in HERA data, Eur. Phys. J. C **78,** 321 (2018).

[66] S. L. Glashow, Resonant scattering of antineutrinos, Phys. Rev. **118,** 316 (1960).

[67] J. G. Learned and S. Pakvasa, Detecting tau-neutrino oscillations at PeV energies, Astropart. Phys. **3,** 267 (1995).

[68] J. F. Beacom, N. F. Bell, D. Hooper, S. Pakvasa, and T. J. Weiler, Measuring flavor ratios of high-energy astrophysical neutrinos, Phys. Rev. D **68,** 093005 (2003); Erratum, Phys. Rev. D **72,** 019901(E) (2005).

[69] E. Bugaev, T. Montaruli, Y. Shlepin, and I. A. Sokalski, Propagation of tau neutrinos and tau leptons through the earth and their detection in underwater / ice neutrino telescopes, Astropart. Phys. **21,** 491 (2004).

[70] L. A. Anchordoqui, H. Goldberg, F. Halzen, and T. J. Weiler, Neutrinos as a diagnostic of high energy astrophysical processes, Phys. Lett. B **621,** 18 (2005).

[71] A. Bhattacharya, R. Gandhi, W. Rodejohann, and A. Watanabe, The Glashow resonance at IceCube: Signatures, event rates and pp vs. $p\gamma$ interactions, J. Cosmol. Astropart. Phys. 10 (2011) 017.

[72] A. Bhattacharya, R. Gandhi, W. Rodejohann, and A. Watanabe, On the interpretation of IceCube cascade events in terms of the Glashow resonance, arXiv:1209.2422.

[73] V. Barger, L. Fu, J. G. Learned, D. Marfatia, S. Pakvasa, and T. J. Weiler, Glashow resonance as a window into cosmic neutrino sources, Phys. Rev. D **90,** 121301 (2014).

[74] A. Palladino, G. Pagliaroli, F. L. Villante, and F. Vissani, Double pulses and cascades above 2 PeV in IceCube, Eur. Phys. J. C **76,** 52 (2016).

[75] J. F. Beacom and J. Candia, Shower power: Isolating the prompt atmospheric neutrino flux using electron neutrinos, J. Cosmol. Astropart. Phys. 11 (2004) 009.

[76] R. Laha, J. F. Beacom, B. Dasgupta, S. Horiuchi, and K. Murase, Demystifying the PeV cascades in IceCube: Less (Energy) is more (Events), Phys. Rev. D **88,** 043009 (2013).

[77] M. G. Aartsen *et al.* (IceCube Collaboration), Energy reconstruction methods in the IceCube neutrino telescope, J. Inst. **9,** P03009 (2014).

[78] S. Palomares-Ruiz, A. C. Vincent, and O. Mena, Spectral analysis of the high-energy IceCube neutrinos, Phys. Rev. D **91,** 103008 (2015).

[79] A. M. Dziewonski and D. L. Anderson, Preliminary reference earth model, Phys. Earth Planet. Inter. **25,** 297 (1981).

[80] See Supplemental Material at http://link.aps.org/supplemental/10.1103/PhysRevLett.122.041101 for details about calculating shower rates in IceCube and the statistical analysis used to extract the cross section.

[81] F. Feroz and M. P. Hobson, Multimodal nested sampling: An efficient and robust alternative to MCMC methods for astronomical data analysis, Mon. Not. R. Astron. Soc. **384,** 449 (2008).

[82] S. R. Kelner and F. A. Aharonian, Energy spectra of gamma-rays, electrons and neutrinos produced at interactions of relativistic protons with low energy radiation, Phys. Rev. D **78,** 034013 (2008).

[83] F. Feroz, M. P. Hobson, and M. Bridges, MultiNest: An efficient and robust Bayesian inference tool for cosmology and particle physics, Mon. Not. R. Astron. Soc. 398, 1601 (2009).

[84] S. Hümmer, M. Rüger, F. Spanier, and W. Winter, Simplified models for photohadronic interactions in cosmic accelerators, Astrophys. J. 721, 630 (2010).

[85] M. G. Aartsen et al. (IceCube Collaboration), Measurement of South Pole ice transparency with the IceCube LED calibration system, Nucl. Instrum. Methods A 711, 73 (2013).

[86] F. Feroz, M. P. Hobson, E. Cameron, and A. N. Pettitt, Importance nested sampling and the MultiNest algorithm, arXiv:1306.2144.

[87] T. P. Robitaille et al. (Astropy Collaboration), Astropy: A community Python package for astronomy, Astron. Astrophys. 558, A33 (2013).

[88] J. Buchner, A. Georgakakis, K. Nandra, L. Hsu, C. Rangel, M. Brightman, A. Merloni, M. Salvato, J. Donley, and D. Kocevski, X-ray spectral modelling of the AGN obscuring region in the CDFS: Bayesian model selection and catalogue, Astron. Astrophys. 564, A125 (2014).

[89] K. Blum, A. Hook, and K. Murase, High energy neutrino telescopes as a probe of the neutrino mass mechanism, arXiv:1408.3799.

[90] M. Bustamante, J. F. Beacom, and K. Murase, Testing decay of astrophysical neutrinos with incomplete information, Phys. Rev. D 95, 063013 (2017).

[91] A. C. Vincent, C. A. Argüelles, and A. Kheirandish, High-energy neutrino attenuation in the Earth and its associated uncertainties, J. Cosmol. Astropart. Phys. 11 (2017) 012.

[92] IceCube Collaboration, Search for contained neutrino events at energies greater than 1 TeV in 2 years of data (2015).

[93] S. Klein (private communication).

[94] Y. Xu, Measurement of high energy neutrino-nucleon cross section of cascade channel with IceCube, Proc. Sci. ICRC2017 (2018) 978.

[95] M. Honda, M. S. Athar, T. Kajita, K. Kasahara, and S. Midorikawa, Atmospheric neutrino flux calculation using the NRLMSISE-00 atmospheric model, Phys. Rev. D 92, 023004 (2015).

[96] E. V. Bugaev, V. A. Naumov, S. I. Sinegovsky, and E. S. Zaslavskaya, Prompt leptons in cosmic rays, Nuovo Cimento C 12, 41 (1989).

[97] P. Gondolo, G. Ingelman, and M. Thunman, Charm production and high-energy atmospheric muon and neutrino fluxes, Astropart. Phys. 5, 309 (1996).

[98] L. Pasquali, M. H. Reno, and I. Sarcevic, Lepton fluxes from atmospheric charm, Phys. Rev. D 59, 034020 (1999).

[99] R. Enberg, M. H. Reno, and I. Sarcevic, Prompt neutrino fluxes from atmospheric charm, Phys. Rev. D 78, 043005 (2008).

[100] T. K. Gaisser, Atmospheric leptons, EPJ Web Conf. 52, 09004 (2013).

[101] A. Bhattacharya, R. Enberg, M. Hall Reno, I. Sarcevic, and A. Stasto, Perturbative charm production and the prompt atmospheric neutrino flux in light of RHIC and LHC, J. High Energy Phys. 06 (2015) 110.

[102] M. V. Garzelli, S. Moch, and G. Sigl, Lepton fluxes from atmospheric charm revisited, J. High Energy Phys. 10 (2015) 115.

[103] R. Gauld, J. Rojo, L. Rottoli, S. Sarkar, and J. Talbert, The prompt atmospheric neutrino flux in the light of LHCb, J. High Energy Phys. 02 (2016) 130.

[104] A. Fedynitch et al., MCE_Q—numerical code for inclusive lepton flux calculations, Proc. Sci., ICRC2015 (2016) 1129.

[105] F. Halzen and L. Wille, Upper limit on forward charm contribution to atmospheric neutrino flux, arXiv:1601.03044.

[106] F. Halzen and L. Wille, Charm contribution to the atmospheric neutrino flux, Phys. Rev. D 94, 014014 (2016).

[107] T. K. Gaisser, Atmospheric Neutrinos, J. Phys. Conf. Ser. 718, 052014 (2016).

[108] A. Bhattacharya, R. Enberg, Y. Seon Jeong, C. S. Kim, M. H. Reno, I. Sarcevic, and A. Stasto, Prompt atmospheric neutrino fluxes: Perturbative QCD models and nuclear effects, J. High Energy Phys. 11 (2016) 167.

[109] R. Engel et al., The hadronic interaction model Sibyll— past, present and future, EPJ Web Conf. 145, 08001 (2017).

[110] S. Schonert, T. K. Gaisser, E. Resconi, and O. Schulz, Vetoing atmospheric neutrinos in a high energy neutrino telescope, Phys. Rev. D 79, 043009 (2009).

[111] T. K. Gaisser, K. Jero, A. Karle, and J. van Santen, Generalized self-veto probability for atmospheric neutrinos, Phys. Rev. D 90, 023009 (2014).

[112] L. A. Anchordoqui et al., Cosmic neutrino pevatrons: A brand new pathway to astronomy, astrophysics, and particle physics, J. High Energy Astrophys. 1–2, 1 (2014).

[113] M. G. Aartsen et al. (IceCube Collaboration), Neutrinos and cosmic rays observed by IceCube, Adv. Space Res. 62, 2902 (2018).

[114] T. Kashti and E. Waxman, Flavoring Astrophysical Neutrinos: Flavor Ratios Depend on Energy, Phys. Rev. Lett. 95, 181101 (2005).

[115] P. Lipari, M. Lusignoli, and D. Meloni, Flavor composition and energy spectrum of astrophysical neutrinos, Phys. Rev. D 75, 123005 (2007).

[116] O. Mena, S. Palomares-Ruiz, and A. C. Vincent, On the Flavor Composition of the High-Energy Neutrino Events in IceCube, Phys. Rev. Lett. 113, 091103 (2014).

[117] M. Bustamante, J. F. Beacom, and W. Winter, Theoretically Palatable Flavor Combinations of Astrophysical Neutrinos, Phys. Rev. Lett. 115, 161302 (2015).

[118] A. C. Vincent, S. Palomares-Ruiz, and O. Mena, Analysis of the 4-year IceCube High-Energy Starting Events, Phys. Rev. D 94, 023009 (2016).

[119] M. G. Aartsen et al. (IceCube Collaboration), Flavor Ratio of Astrophysical Neutrinos above 35 TeV in IceCube, Phys. Rev. Lett. 114, 171102 (2015).

[120] K. Murase, M. Ahlers, and B. C. Lacki, Testing the hadronuclear origin of PeV neutrinos observed with Ice-Cube, Phys. Rev. D 88, 121301 (2013).

[121] K. Murase, D. Guetta, and M. Ahlers, Hidden Cosmic-Ray Accelerators as an Origin of TeV-PeV Cosmic Neutrinos, Phys. Rev. Lett. 116, 071101 (2016).

[122] S. R. Kelner, F. A. Aharonian, and V. V. Bugayov, Energy spectra of gamma-rays, electrons and neutrinos produced at proton-proton interactions in the very high energy regime, Phys. Rev. D **74,** 034018 (2006); Erratum, Phys. Rev. D **79,** 039901(E) (2009).

[123] G. Aad *et al.* (ATLAS Collaboration), Search for strong gravity signatures in same-sign dimuon final states using the ATLAS detector at the LHC, Phys. Lett. B **709,** 322 (2012).

[124] S. Chatrchyan *et al.* (CMS Collaboration), Search for microscopic black holes in pp collisions at $\sqrt{s} = 7$ TeV, J. High Energy Phys. 04 (2012) 061.

[125] M. P. Kowalski, Search for neutrino induced cascades with the AMANDA-II detector, Ph.D. thesis, Humboldt Univeristy, Berlin, 2004.

[126] S. W. Li, M. Bustamante, and J. F. Beacom, Echo technique to distinguish flavors of astrophysical neutrinos, arXiv:1606.06290.

[127] M. G. Aartsen *et al.* (IceCube Collaboration), Searches for extended and point-like neutrino sources with four years of IceCube data, Astrophys. J. **796,** 109 (2014).

[128] M. G. Aartsen *et al.* (IceCube Collaboration), Constraints on Galactic neutrino emission with seven years of IceCube data, Astrophys. J. **849,** 67 (2017).

[129] A. Neronov and D. V. Semikoz, Evidence the Galactic contribution to the IceCube astrophysical neutrino flux, Astropart. Phys. **75,** 60 (2016).

[130] P. B. Denton, D. Marfatia, and T. J. Weiler, The Galactic contribution to IceCube's astrophysical neutrino flux, J. Cosmol. Astropart. Phys. 08 (2017) 033.

[131] M. G. Aartsen *et al.* (IceCube Collaboration), IceCube-Gen2: A vision for the future of neutrino astronomy in Antarctica, arXiv:1412.5106.

[132] S. Adrian-Martinez *et al.* (KM3Net Collaboration), Letter of intent for KM3NeT 2.0, J. Phys. G **43,** 084001 (2016).

[133] M. G. Aartsen *et al.* (IceCube Collaboration), Measurements using the inelasticity distribution of multi-TeV neutrino interactions in IceCube, arXiv:1808.07629.

[134] L. A. Anchordoqui, C. A. Garcia Canal, H. Goldberg, D. G. Dumm, and F. Halzen, Probing leptoquark production at IceCube, Phys. Rev. D **74,** 125021 (2006).

[135] M. Ribordy and A. Y. Smirnov, Improving the neutrino mass hierarchy identification with inelasticity measurement in PINGU and ORCA, Phys. Rev. D **87,** 113007 (2013).

[136] L. N. Lipatov, Reggeization of the vector meson and the vacuum singularity in nonabelian gauge theories, Yad. Fiz. **23,** 642 (1976) [Sov. J. Nucl. Phys. **23,** 338 (1976)].

[137] E. A. Kuraev, L. N. Lipatov, and V. S. Fadin, Multi—Reggeon processes in the Yang-Mills theory, Zh. Eksp. Teor. Fiz. **71,** 840 (1976) [Sov. Phys. JETP **44,** 443 (1976)].

[138] E. A. Kuraev, L. N. Lipatov, and V. S. Fadin, The Pomeranchuk singularity in nonabelian gauge theories, Zh. Eksp. Teor. Fiz. **72,** 377 (1977) [Sov. Phys. JETP **45,** 199 (1977)].

[139] I. I. Balitsky and L. N. Lipatov, The Pomeranchuk singularity in quantum chromodynamics, Yad. Fiz. **28,** 1597 (1978) [Sov. J. Nucl. Phys. **28,** 822 (1978)].

[140] F. Gelis, E. Iancu, J. Jalilian-Marian, and R. Venugopalan, The color glass condensate, Annu. Rev. Nucl. Part. Sci. **60,** 463 (2010).

[141] E. M. Henley and J. Jalilian-Marian, Ultra-high energy neutrino-nucleon scattering and parton distributions at small x, Phys. Rev. D **73,** 094004 (2006).

[142] L. A. Anchordoqui, A. M. Cooper-Sarkar, D. Hooper, and S. Sarkar, Probing low-x QCD with cosmic neutrinos at the Pierre Auger observatory, Phys. Rev. D **74,** 043008 (2006).

[143] V. Bertone, R. Gauld, and J. Rojo, Neutrino telescopes as QCD microscopes, arXiv:1808.02034.

[144] P. Allison *et al.*, Design and initial performance of the Askaryan Radio Array prototype EeV neutrino detector at the South Pole, Astropart. Phys. **35,** 457 (2012).

[145] P. Allison *et al.* (ARA Collaboration), First constraints on the ultra-high energy neutrino flux from a prototype station of the Askaryan Radio Array, Astropart. Phys. **70,** 62 (2015).

[146] P. Allison *et al.* (ARA Collaboration), Performance of two Askaryan Radio Array stations and first results in the search for ultrahigh energy neutrinos, Phys. Rev. D **93,** 082003 (2016).

[147] S. W. Barwick, ARIANNA: A new concept for UHE neutrino detection, J. Phys. Conf. Ser. **60,** 276 (2007).

[148] S. W. Barwick *et al.* (ARIANNA Collaboration), A first search for cosmogenic neutrinos with the ARIANNA hexagonal radio array, Astropart. Phys. **70,** 12 (2015).

[149] J. Alvarez-Muiz *et al.* (GRAND Collaboration), The Giant Radio Array for Neutrino Detection (GRAND): Science and design, arXiv:1810.09994.

[150] A. V. Olinto *et al.*, POEMMA: Probe Of Extreme Multi-Messenger Astrophysics, Proc. Sci., ICRC2017 (**2017**) 542.

[151] L. A. Anchordoqui, Z. Fodor, S. D. Katz, A. Ringwald, and H. Tu, Upper bounds on the neutrino-nucleon inelastic cross section, J. Cosmol. Astropart. Phys. 06 (2005) 013.